

# Acoustic Blower Using Fluidic Diodes and a Nonuniform Resonator

Sonu K. Thomas\* and T. M. Muruganandam

Department of Aerospace Engineering, Indian Institute of Technology Madras,  
Chennai 600036, India.

## ABSTRACT

Performance of a nonuniform rectangular resonator coupled with fluidic diodes as an acoustic blower was investigated. Nonuniform resonator with a linear area variation was used to achieve high amplitude pressure at the small end of the resonator, where the diodes were located. Experiments were done with pairs of diodes with 1, 2, 3, 4 and 5 diode elements in series. The diode elements used had two different nozzle diameters but same length. The volume flow rate and pressure were measured for each case by bubble flow method for zero back pressure case, and tank filling method for non-zero back pressure cases. It was found that higher driving amplitudes gave higher flow rates and higher load capacity. Increasing the number of diode elements also did the same except for small diode diameter cases, where the blower offers higher load bearing capacity at higher loads and lower flow rates at lower loads. The measured maximum peak pressure was 15.9 kPa and the maximum flow rate observed was 11.07 L/min of air respectively, while operating around 940 Hz.

## 1. INTRODUCTION

Valveless pumping is an exciting field of research in view of its many applications. A review by Tesar [1] gives details of different types of valveless pumping principles in a comprehensive manner. Two of the most commonly used valveless pumping principles are, valveless impedance pumping [2–4] and valveless reciprocating pumping [5–9]. In case of valveless impedance based pumping the flow rectification is achieved by connecting two tubes with different impedance, one of which is pinched periodically. The periodic pinching produces travelling wave which then reflects where the impedance of the tube changes, thus producing net flow. While, in case of a valveless reciprocating pump, an oscillating chamber volume is connected to two diffuser/nozzle elements, which in turn rectifies the flow. Most of the above mentioned pumps have been tested for pumping liquids.

Recently, a new type of pump referred to as valveless standing wave pump (SWP) was investigated by Nabavi *et al.* [10] and Nabavi and Mongeau [11]. Nabavi *et al.* [10] showed that pumping is directly proportional to the standing wave pressure amplitude at pressure antinode. There already existed other standing wave pumps which used uniform resonators [12–14]. These previously proposed SWPs used one or more check valves for their operation and, therefore, moving mechanical components are built-in. Moreover, all these resonators were uniform cross section ducts which limit the maximum obtainable peak pressure at resonance. It is well known fact that shocks form inside the uniform tube when the gas is oscillating at one of its resonance frequencies. Shock formation limits the amount of energy that can be put into the standing wave [15].

Lucas *et al.* [16, 17] in 1999 using resonant macrosonic synthesis technology (RMS) demonstrated the generation of high amplitude standing wave in a nonuniform resonator. They too used reed type mechanical valve for the rectifying the oscillating flow. Problems associated with these mechano-fluidic devices include fatigue of moving valves, failure due to wear and tear and operation only at low driving frequencies. Usually, the term ‘pump’ is used for liquids, and ‘blower’ for gases. Even though some authors in the literature have used the term ‘pump’ for air as the working fluid [9, 10], the present authors prefer to use the term ‘blower’ for their device, as the pumped fluid is air.

There are many known no moving part rectifying elements in the literature that can perform rectification. These rectifiers cannot close off the return flow completely. Nevertheless, their reliability

---

\*Corresponding author: thomas.sonu91@gmail.com

and simplicity makes them a suitable choice for oscillatory flow rectification, besides being less expensive to manufacture, easy to produce in different scales (ranging from micro to macro sizes) and having long operating life. Yastrebova [18] and Priestman and Tippetts [19] discuss different types of rectifiers. The oldest among these diodes has to be one by Tesla in 1920 [20]. The rectifying element (sometimes called 'fluidic diode', or 'dynamic passive valve', etc) can look like a convergent/divergent duct. Stemme and Stemme [5] used convergent/divergent elements as diodes. Gerlach *et al.* [6] used truncated pyramid channels as diodes instead. Forster *et al.* [21] used a valvular conduit bifurcating a channel flow as diode, which was a modification to Tesla's design. Olsson *et al.* [7] numerically and experimentally studied flat-walled diffuser elements as a rectifying device for valveless micropumps. Another type of fluidic valve called as jet type rectifier with attachment to curved wall works in a travelling wave mode. This type of valve was used to pump extremely dangerous liquids [22]. Also, this idea came to be known as forward flow diverter (FFD), uses Coanda effect to move air in a no moving part blower [23]. Several computational efforts have been focused on understanding the rectification process by the fluidic diodes [24–26].

Fluidic diodes have directional asymmetry along the flow direction, which results in directional pressure drop. One of the major contributors to this pressure drop is 'minor loss' associated with sudden change in flow direction and transition between channels [27–31]. The minor loss for a sudden expansion is different from that for a sudden contraction. A jet pump develops an adverse pressure gradient using the minor loss concept. Swift *et al.* [32] made use of a jet pump to suppress, unwanted streaming in a traveling wave engine and refrigerator. The present study exploits minor loss phenomena to produce a steady pressure difference across a fluidic element.

The present study explores the possibility of enhancing valveless standing wave blower for air with nonuniform resonators, which produce high amplitude standing wave. The idea is to enhance the pumping by combining a nonuniform resonator and no moving part rectifying elements. The present study brings two new modifications to the existing principles; the resonator shape used, and the diode configurations. In the present study, the fluidic diode was a series of one or more convergent/divergent fluidic elements arranged in series. Focus is on understanding the effectiveness of these fluidic elements, when they are arranged in series. Performance is measured in terms of net flow rate produced by the blower.

## 2. EXPERIMENTAL SETUP

Figure 1(a) shows the schematic of the experimental setup. In this study a nonuniform rectangular cross section duct with linear area variation, was used as an acoustic compressor. The linear variation is given by Eqn.1 below; with the width of the duct maintained constant at 5 cm. Bottom portion is attached to an acoustic horn driver unit (Capital 2165/150W) which has diaphragm diameter 35 mm. The driver unit was driven by power amplifier (AHUJA SSA-350). The frequency and amplitude of vibration of diaphragm are controlled using a function generator (Tektronix AFG 30220B) and the power amplifier. Dynamic pressure transducer (PCB model 113B27) is used to measure dynamic pressure at the small end of the resonator.

$$A(x) = (ax + b), \quad \text{where } a = 2.25 \text{ cm}, b = 10 \text{ cm}^2 \text{ and } 0 \leq x \leq 20 \text{ cm} \quad (1)$$

In this study, positive displacement based bubble flow meter as shown in Fig 1(b) was used to measure flow rates. This is a primary standard flow meter with zero back pressure. Squeezing of the bulb causes soap solution to momentarily rise and cover the tip of the graduated cylinder. Air flowing into the base of flow meter forces the soap film to rise in the cylinder. Thus by timing the rise of soap film between calibrated volume marks, volume flow is obtained. These type flow meters operate at virtually the same pressure and temperature, no pressure and temperature correction is needed. High speed camera (IDT N4-S3) was used to measure the rate of rise of soap film. It was also noted from high speed imaging that the soap film was not distorted due to acoustics. Another method was used to measure flow rates at different non-zero back pressures. Here, the resonator and fluidic diode assembly was connected to a pressure tank as shown in Fig 1(c). The outflow to be measured is connected to the pressure tank. Omega PXI-140 series, solid state piezoresistive pressure sensor was used to monitor the pressure rise in the tank. The resonator was at atmospheric pressure at the beginning of the experiment, when the driver is started. Rate of change of pressure in the tank was used to deduce instantaneous incoming mass flow rate of air. Care was taken to ensure that the amplifier delay (due to sudden starting of the amplifier) was minimised, and the driver starts

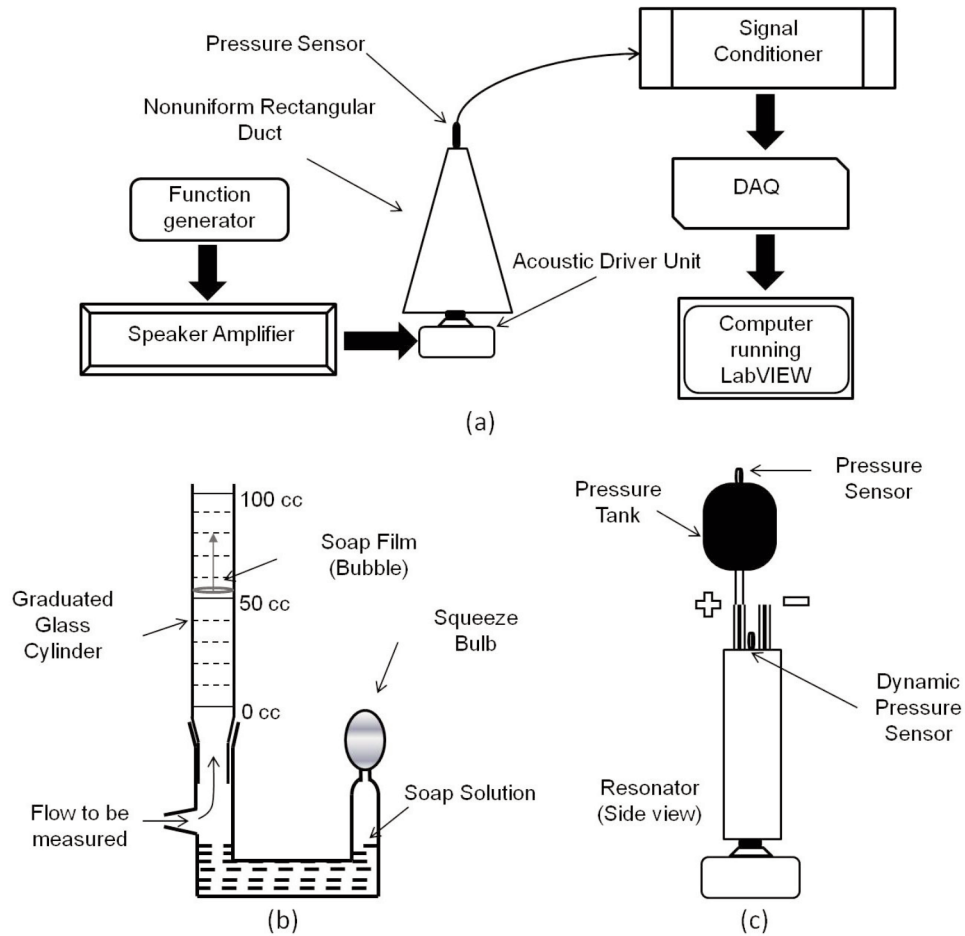


Figure 1. (a) Schematic of the experimental setup, (b) Schematic of bubble flow meter and (c) Schematic of resonator and fluidic diode assembly connected to a pressure tank.

instantaneously at the driving voltage. However, the peak pressure in the resonator took around 20 msec to come to steady state.

Each diode set (the pair of diodes) mounted on the acoustic compressor was arranged as shown in Fig. 2. One diode was arranged in a positive configuration indicated by a '+' sign (here after D1) and another diode in negative configuration indicated by a '-' sign (here after D2). Sign convention used here is consistent with Gerlach *et al.* [6].

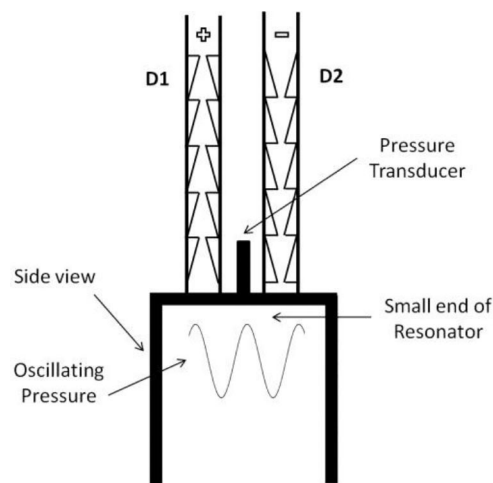


Figure 2. Fluid diodes coupled to small end of the resonator.

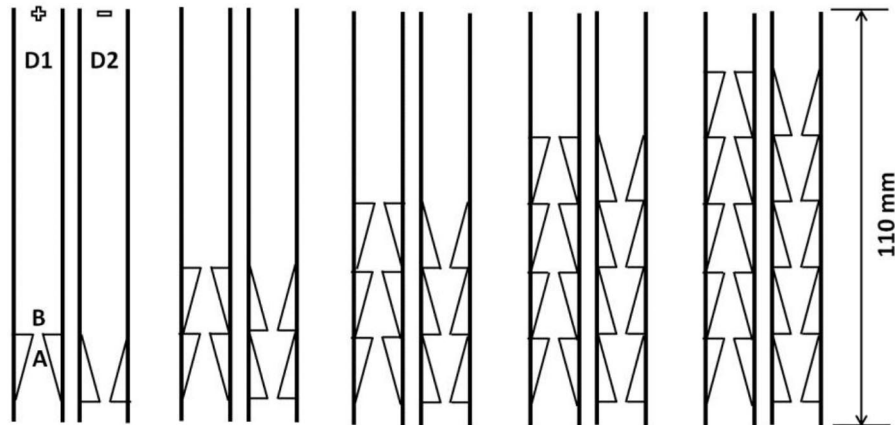


Figure 3. Five fluidic diode pair configurations used in the present study (note that all these configurations are axisymmetric).

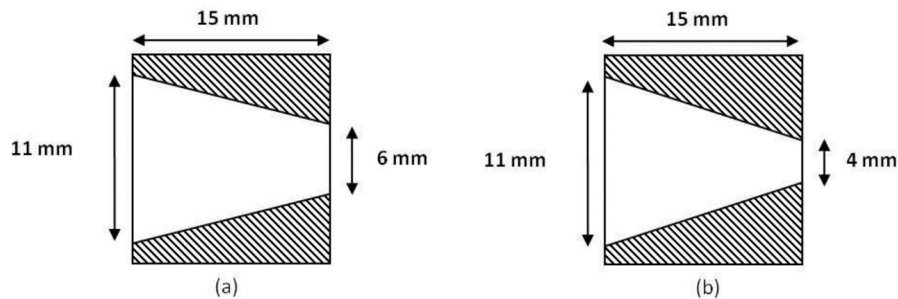


Figure 4. Two different individual axisymmetric diode elements used in the present study. (a) 6 mm diode element, (b) 4 mm diode element.

Five pairs of fluidic diodes as shown in Fig. 3 were used in this study. The diode tubes were made of individual convergent diode elements (see Fig. 4), glued together in series and rest of the length by plain tubes of 11 mm ID. The five different diode pair configurations were made with all identical diode elements, but two different such sets were made for the two diode elements shown in Fig. 4. These diode configurations will be referred to by the throat size of the individual diode elements used. From the results that will be presented in following sections, Reynolds number ( $Re$ ) in the diode passage varies from 225 (in 11 mm passage for lowest flow rate) to 3380 (in 4 mm passage for highest flow rate case) and Shrouhal number ( $St$ ) varies from 0.28 (in 4 mm diode case for highest flow rate) to 32 (in 11 mm passage for lowest flow rate).

### 3. RESULTS AND DISCUSSIONS

Experiments were conducted for all the diode pairs for various sinusoidal driving amplitudes at fundamental frequency, ensuring the ambient conditions did not change. Pressure and flow rate measurements were recorded after the initial transients settled down. This was typically a few acoustic cycles. Each data was recorded for four seconds and the results were found to be steady even for longer times, and repeatable.

#### 3.1. Effect of Different Diode Configurations on Resonance Frequency of the Resonator

For a given driving amplitude, the peak pressure of the standing wave at the small end was measured at different frequencies. The frequency with the maximum peak pressure was defined as resonance frequency. The different end boundary conditions also had a minor effect on the resonance frequency of the duct as shown in Fig. 5. However, the change in frequency was only around 1%. The difference between the resonance frequency values for 4 mm and the 6 mm diode elements also were found to be less than 0.5%. Thus the changes in configurations do not change the acoustic characteristics of the resonator much. Nevertheless, it was observed that the frequencies for the 6 mm diodes were all higher

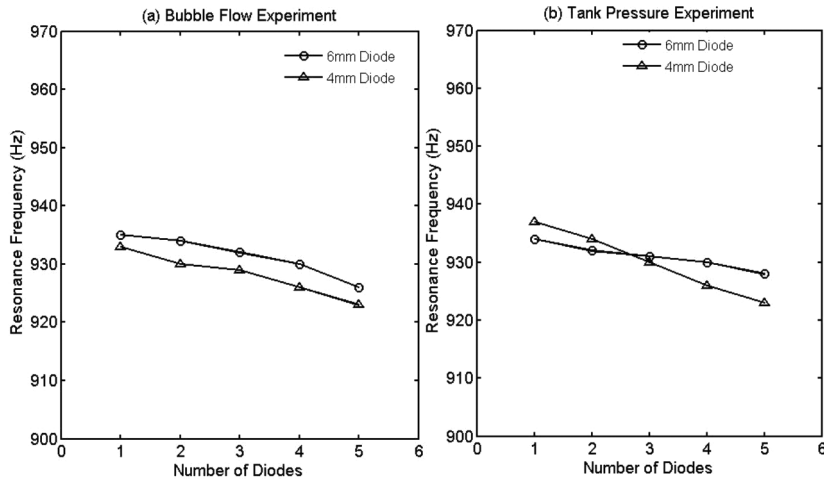


Figure 5. Resonance frequency versus number of diodes in series. Results from (a) bubble flow experiments, and (b) tank pressure experiment. Error bars are smaller than the markers.

than the corresponding configurations with 4 mm diodes during the zero back pressure flow experiments. When the same experiments were performed with the tank connected to ‘D1’, the trend in the difference between 4 mm and 6 mm diode cases switched for the 1 and 2 diode element cases.

**3.2. Effect of Different Diode Configurations on Peak Pressure of the Standing Wave**

Figure 6 shows peak pressure for different pairs of diodes, at the small end of the resonator, for the different driving amplitudes. This pressure can be considered as inlet condition to the diodes. It should be noted that, resonator end boundary condition is altered due to the presence of fluidic diodes. Figure 6 (a) corresponds to bubble flow measurement experiment. There is only a slight variation of peak pressures with change in number of diodes, as is evident from the plot. The pressure amplitudes increased with the driving voltage, as expected. One can notice the high values of peak pressures of 16 kPa in this resonator at 40 V driving voltage. It can be as high as 35 kPa without diodes (rigid closed end resonator). This is possible only for nonuniform resonators [17]. It can be seen that the 6mm diode configurations show slightly higher peak pressures compared to the corresponding 4mm diode configurations (with only one exception). It appears that the peak pressures for 6mm diodes are higher than those for 4mm diodes, which is in line with trend in resonance frequencies between these cases. This suggests that the 6 mm diodes give a slightly more closed end type boundary condition for the resonator than the 4 mm diodes.

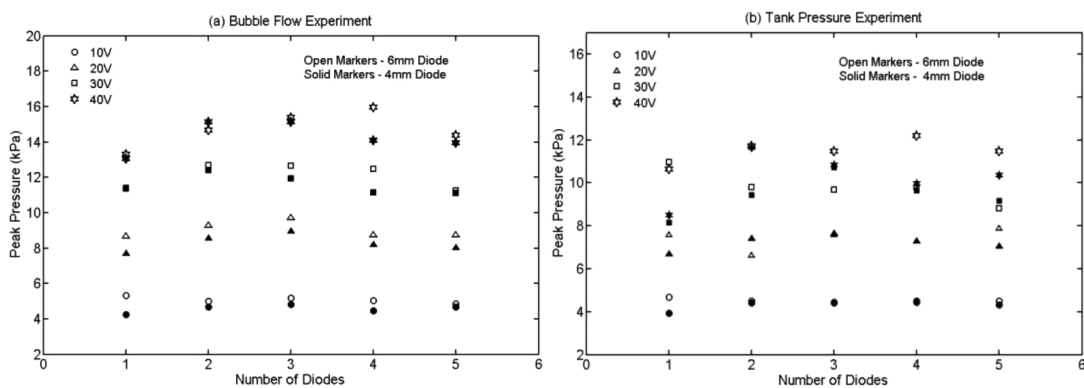


Figure 6. Effect of number of diodes on peak pressure for different diode configurations. Results from (a) bubble flow measurement (zero load condition), and (b) tank filling measurement near saturation of the tank (maximum load condition). Error bars for the pressure data are smaller than the markers.

Figure 6 (b) presents data from tank filling experiment, when the tank pressure has saturated, which corresponds to full load for the blower. In case of tank pressure measurement experiments, the peak pressures for most of the cases have lower peak pressures than their counterparts in bubble flow experiments. In general, even here, the 6 mm diode configurations gave higher peak pressures than 4 mm diode configurations.

### 3.3. Effect of Different Diode Configurations on Zero Load Flow Rate

Volume flow measurements were done only for 'D1' at different driving amplitudes (10–40 V) and for different sets of diodes. Figure 7 shows the flow rates measured at zero load condition. One can notice high values of flow rates around 11 L/min at 40 V driving voltage. A slight variation of flow rates (max of 12%) with change in number of diodes is evident from the plot. This suggests that single diode itself is effective enough in the rectification process and adding further diodes does not significantly improve the performance. The flow rates increased with the driving voltage, as expected. However, the trend was not the same as that seen in Fig. 6, suggesting that there is some other effect than just the peak pressure dependence.

### 3.4. Effect Peak Pressure of Resonator on Zero Load Volume Flow Rate

Figure 8 shows effect of peak pressure on the flow rate. It is evident that the flow rate at zero load increases as the peak pressure of the resonator increases. This is similar to trends observed by Nabavi *et al.* [10], who used uniform resonator with conical diode. However, they reported only two data points. The flow rates

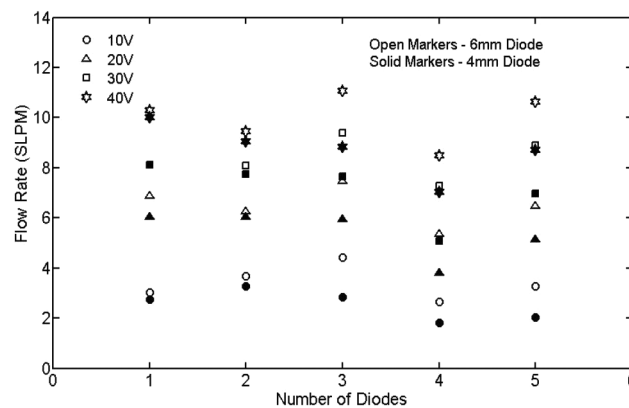


Figure 7. Effect of number of diodes on flow rates induced by different diode configurations. All measurements were for zero back pressure conditions. Error bars for the flow rate data are smaller than the markers.

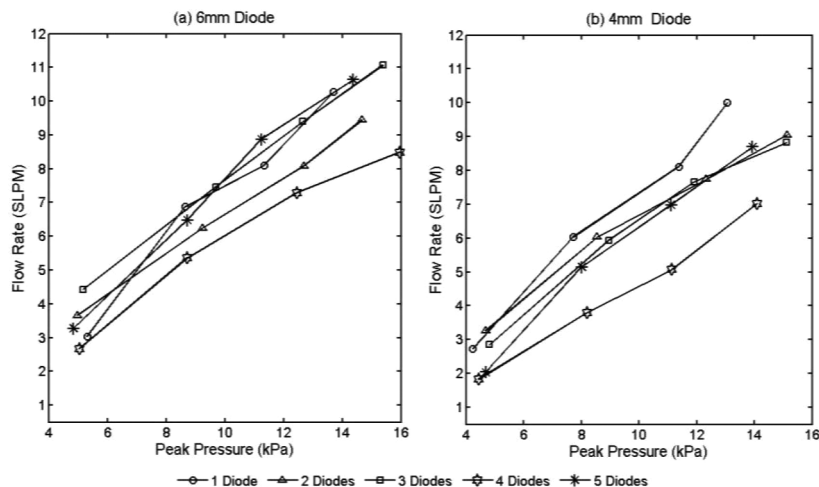


Figure 8. Flow rate vs. peak pressure at zero load for different diode configurations.

achieved in this study are order of magnitude higher than that obtained by Nabavi *et al.* [10]. They obtained maximum flow rate 606 mL/min of air at peak pressure of 535 Pa. In the present study, flow rates of the order 11070 mL/min of air have been achieved at peak pressure of 15400 Pa. The marked improvement in flow rates is solely due to the increased peak pressure. This higher peak pressure was achievable only due to the nonuniform resonator.

While the flow rate increases with peak pressures in the resonator, the trend is not exactly the same for different diode configurations. This suggests that there is a secondary effect due to the diode configurations. It is conjectured that the end boundary conditions for the resonator and flow resistance in the diode passage are modified by the diode configurations, causing the secondary effects.

**3.5. Flow Rate Measurements From Tank Filling Experiments (Non-Zero Load Behavior)**

The outlet of the blower is connected to a sealed pressure tank of a known volume, and the increase in pressure is monitored. Rate of change of pressure in the tank was used to deduce instantaneous incoming mass flow rate of air. Figure 9 presents the tank pressure time traces for all diode configurations at 40 V driving. It should be noted that the pressure trace shows only the mean pressures from the sinusoidal pressure traces. The pressure in the tank increases almost linearly and then plateaus off after some time. The flow rates deduced from this pressure variation shows almost constant flow rate up to 50 msec and after that, it decreases to zero monotonically, for all configurations. The bottom plots in Fig. 9 show the blower characteristics at non-zero back pressures. It can be noted that the almost linear drop in the flow rates with increase in back pressure is an expected blower performance.

However, there is an almost constant portion in blower characteristics, which is abnormal especially at lower back pressures. It can be seen from the figure that for all the configurations, the flow rate is constant or slightly increasing for the first  $50 \pm 3$  msec, and after that, it gives decreasing flow rates. The same temporal behavior was observed for other driving voltages as well. Authors believe that this may be due to both the delay in achieving steady state in resonator (after the acoustic driver starts) and the filling process of the tank itself, as these are the only invariants across these cases. The resonator takes around 20 msec to reach steady state. The Helmholtz time period for the tank is around 30 msec, suggesting that the tank pressure based flow rate measurements may not be reliable for the first Helmholtz period. To the best of authors' knowledge there is no observation of this kind in the literature, to corroborate. Thus, the flat portion of the blower characteristics will be ignored in this work. This causes the number of data points before saturation of the tank pressure to be low for low driving conditions.

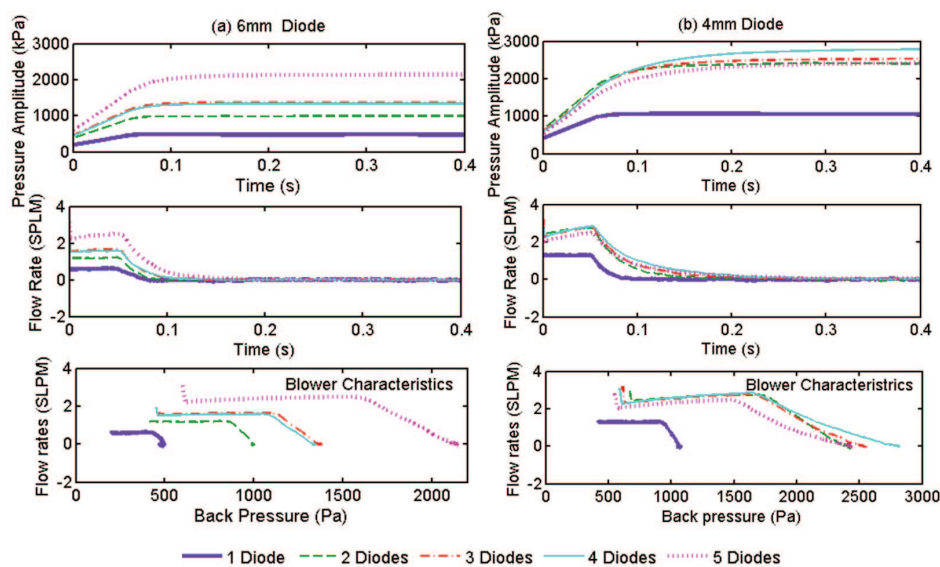


Figure 9. Tank pressure and flow rate time traces, and blower characteristics deduced from it for 6 mm diode and 4 mm diode respectively.

### 3.6. Overall Blower Characteristics

A blower is typically characterised by its performance under different back pressure conditions. The previous sections gave the blower performance from two different measurement methods. This section presents the data for both zero and non-zero back pressure conditions (see Fig. 10), for all the diode configurations, at different driving voltages. The lines on the plots are linear fits of data from the tank filling method (ignoring the flat portion of data). It can be seen that the lines are not very close to the zero load measurements for each of the cases. This is yet to be explained. However, these lines will be considered to be the blower characteristics for each configuration and driving voltage, as measured from the unsteady filling of the tank.

Figure 10(a) shows blower characteristics for 6 mm diode configurations. Clear distinction in the blower characteristics can be observed across configurations with different numbers of diode elements, and across different driving amplitudes. It is clear that the flow rates at given back pressure increases as the number of diode elements increases. Only for 3 and 4 diode element data the trend seem to have switched in the case of 10 V and 30 V. It is interesting to note that higher number of diodes are able to handle higher back pressure for a given flow rate, and supply higher flow rate for a given back pressure. The data for different drive amplitudes shows that flow rates as well as the back pressures increase as the drive amplitude increases. It should be noted that the same is not true for zero load condition, as observed earlier in Fig. 7. Another interesting observation is that for a 1 diode element case the blower characteristic is way off when compared with the zero load condition. This may be due to the lower back pressure, giving very few data points from the tank pressure rise based measurement.

Figure 10(b) shows blower characteristics for 4 mm diode configurations. There is no clear distinction between the blower characteristics for different diodes (above 2) cases unlike 6 mm diode cases. Only 1 & 2 diode element cases look distinct compared to higher number diode case. The 1 diode element 4 mm case could withstand higher back pressure for a given flow rate, and also can pump higher flow rate for a given back pressure compared to 1 diode element 6 mm case. The same is observed for 2 diode element 4 mm configurations, with lesser increase in flow rates. The best performance curve for 4mm diode case is achieved for the 2 diode elements case. In both Figs. 10 (a and b), higher driving increases the saturated back pressure. Further, the saturated back pressure increases with increase in number of diodes for a given driving for 6 mm cases, and this is true for 4mm cases only up to 2 diode elements.

The 4 mm diode configurations have lower flow rate for zero back pressure at same driving, compared to 6 mm diodes. This may be due to dominant friction effects in the 4 mm passage formed between each diode element. However, 4 mm diode configurations apparently can handle higher back pressures supplying the same flow rate, at same driving, compared to 6 mm diode configurations. This is in spite of peak pressures for 6 mm diode cases being higher. This suggests that the smaller diode hole size helps in pumping against back pressure. It is evident that adding more number of diode elements in the case of 4 mm diode is ineffective. This may be because of friction decreasing the flow rate through longer 4 mm passage available for the flow, when more diode elements are added. In case of 6mm diode configurations, increasing the number of diode elements still increases the performance, suggesting lesser friction effects.

It can be summarised that the smaller hole size helps handle high load conditions for the same flow rate with given driving, but giving lower flow rates for low load conditions. Increasing the number of diode elements increases the performance both in terms of back pressure and flow rate, except when the hole sizes are small where friction is dominant. Higher driving amplitudes lead to higher peak pressures and thus higher flow rates and higher load rating. While increase in peak pressures increases performance, increase in number of diode elements does not guarantee increase in peak pressures. This suggests that there are coupling effects between the number of diodes causing end boundary condition changes to the resonator, and the friction in the diode flow passage.

### 3.7. Uncertainty Analysis

The PCB piezoelectric transducer employed for pressure measurements in the resonator has a resolution of 0.007 kPa and an uncertainty of  $\leq 1\%$  of full scale. The ambient conditions (30°C and 77% relative humidity) are nearly constant with a maximum temperature variation of  $\pm 1^\circ\text{C}$  and  $\pm 2\%$  variation in relative humidity. The frequency resolution based on the FFT (Fast Fourier Transform) is 0.33 Hz. The flow rate measurements from bubble flow experiments had an uncertainty of 0.9%.

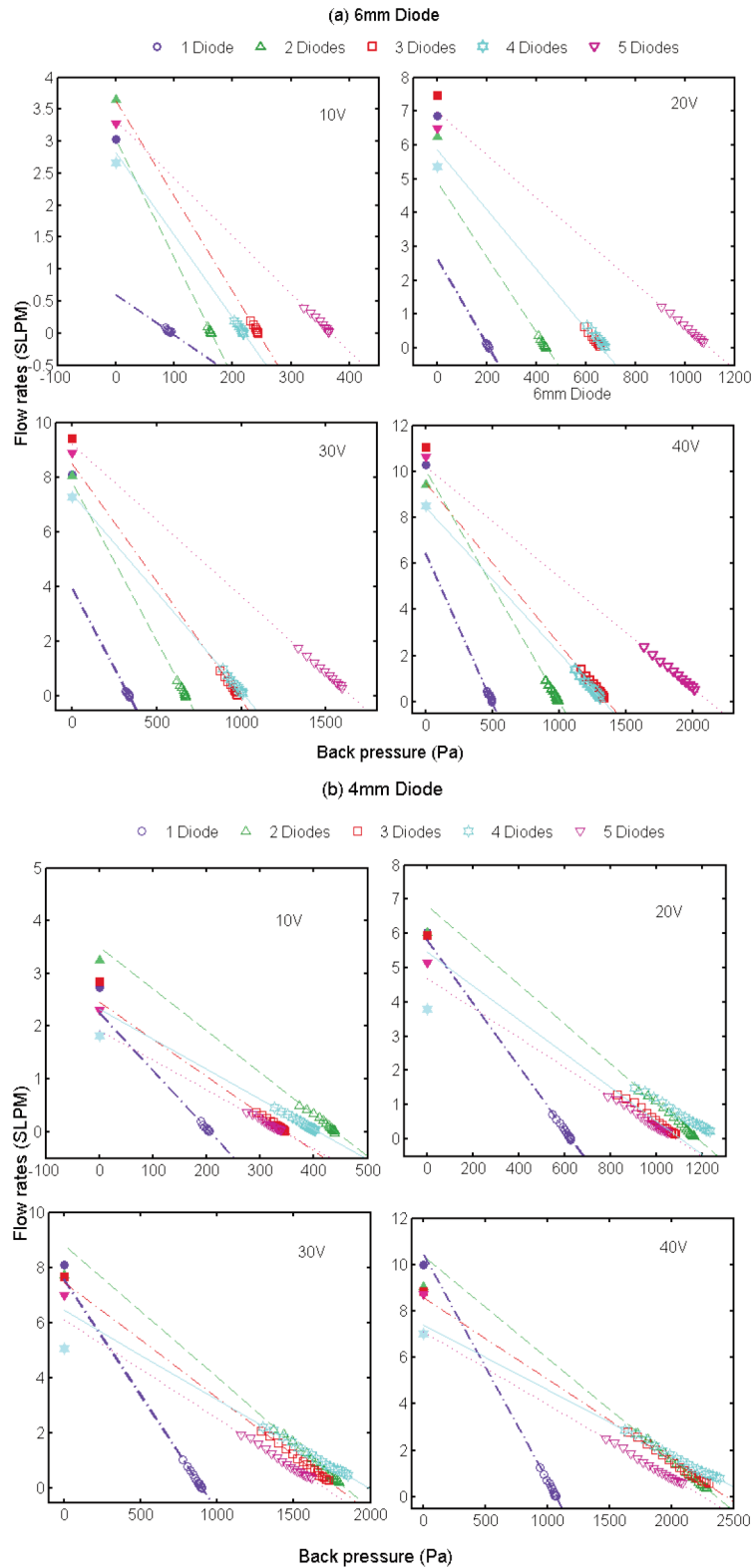


Figure 10. Blower characteristics (a) 6 mm diode elements and (b) 4 mm diode elements. Error bars are smaller than the markers.

Omega PX143 series transducer used in tank pressure measurement has a resolution of  $\pm 13$  Pa. The flow rate measurements from tank pressure based measurement have an uncertainty of 1%. All these uncertainty values are smaller than the marker sizes used in the presented data.

#### 4. CONCLUSION

In this work, a nonuniform rectangular resonator was used to produce high amplitude standing waves and fluidic diodes were used to rectify the oscillating flow to form an acoustic blower. The resonator used had a linear area variation, and the diodes were placed at the small end of the resonator. Experimental study was conducted for a series arrangement of different diode elements. Two different flow measurement methods were used to measure flow rates for zero and non-zero back pressure conditions. Experiments show that the resonant frequencies were not affected appreciably for different diode configurations. Increasing the number of diode elements increases the performance both in terms of back pressure and flow rate, except when the hole sizes are small, where friction is dominant. While smaller hole diodes give higher flow rates performance at higher loads, they deliver lower flow rates at lower load conditions. Higher driving amplitudes lead to higher peak pressures and thus higher flow rates and higher load bearing capacity.

It was found that this device could produce net flows of the order of 11 L/min of air while operating around 940 Hz. Thus, fluidic diodes can be used as an alternative to the mechanical valves in existing standing wave pumps for flow rectification. This flow rate is higher than that produced by most other valveless acoustic pumps of comparable size, due to higher peak pressures achieved by the nonuniform resonator. Thus, a combination of a nonuniform standing wave resonator and fluidic valves can constitute an acoustic blower. These results are encouraging and can be applied to acoustic compressors based on RMS technology for flow rectification.

#### REFERENCES

- [1] V. Tesar, 2008. Valve-less rectification pumps. In: *Dongqing, L. (Ed.), Encyclopedia of Microfluidics and Nanofluidics. Springer Science + Business Media*, p. 2132, ISBN: 978-0-387-48998-8.
- [2] A. I. Hickerson, D. Rinderknecht, and M. Gharib, Experimental study of the behavior of a valveless impedance pump, *Exp. Fluids* 38, 534 (2005).
- [3] G. Manopoulos, D. S. Mathioulakis, and S. G. Tsangaris, One dimensional model of valveless pumping in a closed loop and a numerical solution, *Phys. Fluids* 18, 017106, 2006.
- [4] A. I. Hickerson, D. Rinderknecht, and M. Gharib, A valveless micro impedance pump driven by electromagnetic actuation, *J. Micromech. Microeng.* 15, 861, 2006.
- [5] E. Stemme, G. Stemme, A valve-less diffuser/nozzle-based pump, *Sensors and Actuators A*, 39, 1993:159–167.
- [6] T. Gerlach, M. Schuenemann, and H. Wurmus, A new micropump principle of the reciprocating type using pyramidal micro flow channels as passive valves, *J. Micromech. Microeng.* 5(2), 1995:199–201.
- [7] A. Olsson, G. Stemme, and E. Stemme, Numerical and experimental studies of flat-walled diffuser elements for valve-less micropumps, *Sensors and Actuators A*, 84, 2000:165–175.
- [8] A. Olsson, G. Stemme, and E. Stemme, A Valve-Less Planar Pump In Silicon, *The 8th International Conference on Solid-State Sensors and Actuators, and Eurosensors IX. Stockholm, Sweden*, June 25–29, 1995.
- [9] A. Olsson, G. Stemme and E. Stemme, The first valve-less diffuser gas pump, *1997 IEEE 10th International Workshop on Micro Electro Mechanical Systems (MEMS'97)*, 1997.
- [10] M. Nabavi, K. Siddiqui, and J. Dargahi, Analysis of the flow structure inside the valveless standing wave pump, *Physics of Fluids*, 20, 2008:126101.
- [11] M. Nabavi and L. Mongeau, Numerical analysis of high frequency pulsating flows through a diffuser-nozzle element in valveless acoustic micropumps, *Microfluid Nanofluid*, 7, 2009:669–681.
- [12] H. Mandorian, Standing wave pump, *U.S. Patent No. 3743446* (3 July 1973).
- [13] R. Bishop, Standing wave pump, *U.S. Patent No. 6079214* (27 June 2000).
- [14] T. Lucas, Standing wave compressor, *U.S. Patent No. 5020977* (4 June 1991).
- [15] R. A Saenger, and G. E. Hudson, Periodic Shock waves in resonating gas columns, *J. Acoust. Soc. Am.* Vol 32, No 8, 1960, pp. 961–970.
- [16] T. Lucas, T. W. Van Doren, Resonant macrosonic synthesis, *U.S. Patent No. 5892293* (April 6, 1999).

- [17] C. C. Lawrenson, B. Lipkens, T. S. Lucas, D. K. Perkins, and T. W. Van Doren, Measurement of macrosonic standing wave in oscillating closed cavities, *J. Acoust. Soc. Am.* 104, 623–636 (1998).
- [18] E. V. Yastrebova, Fluid diodes (review), *Automatika i Telemekhanika*, 3, 1971:101–106 (in Russian).
- [19] G. H. Priestman, and J.R. Tippetts, Factors affecting the application of vortex diodes and throttles, *Proceedings of the Symposium Fluid Control and Measurement (FLUCOME)*, Pergamon Press, Oxford, 1985:241–246.
- [20] N. Tesla, Valvular conduit, *US Patent No. 1,329,559* (1920).
- [21] F. K. Forster, R.L. Bardell, M.A. Afromowitz, N.R. Sharma, and A. Blanchard, Design, fabrication and testing of fixed-valve micro-pumps, *Proceedings of the ASME Fluids Engineering Division ASME*, vol. 234, IMECE, 1995:39–44.
- [22] V. Tesar, Pump for extremely dangerous liquids, *Chem. Eng. Res. Des.*, Volume 89, 8 December 2011, Pages 940–956.
- [23] V. Tesar, Development of a no-moving-part blower for difficult operating conditions, *Chem. Eng. Res. Des.*, Volume 91, Issue 12, December 2013, Pages 2401–2411.
- [24] Y. C. Wang, J. C. Hsu, P. C. Kuo, and Y. C. Lee, Loss characteristics and flow rectification property of diffuser valves for micropump applications, *International Journal of Heat and Mass Transfer*, 52 (2009), 328–336.
- [25] V. Singhal, S. V. Garimella, and J. Y. Murthy, Low Reynolds number flow through nozzle-diffuser elements in valveless micropumps, *Sensors and Actuators A*, 113, 2004: 226–235.
- [26] C. C. Hsu, Y. T. Chen, M. C. Chang, and S. W. Kang, Numerical Studies of Curved-walled Micro Nozzle/Diffuser, *Nano/Micro Engineered and Molecular Systems*, 2006, NEMS '06.
- [27] I. E. Idelchik, Handbook of hydraulic resistance, *CRC Press*, 1994.
- [28] B. Said and J. M. Philip, Acoustic streaming: From Rayleigh to today, *Aeroacoustics*, vol. 2 nos. 3 & 4 (2003).
- [29] P. J. Morris, S. Boluriaan and C. M. Sheih, Numerical simulation of minor losses due to a sudden contraction and expansion in high amplitude acoustic resonators, *Acta Acustica united with Acustica*, 90, 2004:393–409.
- [30] M. Mironov, V. Gusev, Y. Auregan, P. Lotton, M. Bruneau and P. Piatakov, Acoustic streaming related to minor loss phenomenon in differentially heated elements of thermoacoustic devices, *J. Acoust. Soc. Am.* 112(2), 2002.
- [31] A. Petculescu and L. A. Wilen, Oscillatory flow in jet pumps: Nonlinear effects and minor losses, *J. Acoust. Soc. Am.* 113(3), 2003.
- [32] G.W. Swift, D. L. Gardner, and S. Backhaus, Acoustic recovery of lost power in pulse tube refrigerators, *J. Acoust. Soc. Am.* 105, 1999:711–724.

